Grid-point and time-step estimates for wall-modeled large-eddy simulation of nonequilibrium flows

By R. Agrawal, S. T. Bose† AND P. Moin

1. Motivation and objectives

One of the ways to assess the feasibility of performing computational fluid dynamics (CFD) analyses is determined by the simulation cost and its *a-priori* estimates. A significant contributor to this cost is the total number of degrees of freedom in the discrete system. This is equivalent to the number of grid points in the computational domain that are required to perform the simulation with reasonable accuracy for the quantities of interest.

Three simulation paradigms are commonly used to study wall-bounded turbulent flows, namely, direct numerical simulation (DNS), wall-resolved large-eddy simulation (WRLES), and wall-modeled large-eddy simulation (WMLES). DNS is an approach in which all the scales of the flow up to the Kolmogorov scales are locally resolved on the computational grid. In the WRLES approach, the important, energy-producing turbulent eddies near the wall are resolved, but the grid is coarsened in the outer flow, and a subgrid-scale model is used to capture the effect of the unresolved scales. As the Reynolds number increases, both these methods, which rely on resolving the near-wall flow, become prohibitively expensive because the dominant turbulent structures become smaller in outer units. Instead, WMLES has become an emerging paradigm in which the entire effect of the near-wall, subgrid flow is modeled as a boundary flux onto the outer flow, typically using a wall model.

Chapman (1979) provided early grid-point estimates for the WMLES paradigm; the cost scaling is reported to be $N_{pts}^{wm} \sim Re_x^{0.4}$ (where N_{pts} is the total number of grid points in the domain, and Re_x is the Reynolds number of the flow based on freestream velocity and a characteristic streamwise length scale). The estimates were based on the power-law assumption, $\delta/x \sim Re_x^{-1/5}$ and $C_f \sim Re_x^{-1/5}$, for flat-plate flows for $Re_x \leq 10^6$. The scaling $N_{pts}^{wm} \sim Re_x^{0.4}$ for WMLES is based on the average boundary layer thickness over a specified streamwise distance. The first set of revisions to Chapman's estimates was provided by Choi & Moin (2012). The authors used the following correlations based on the experimental results from Nagib *et al.* (2007) and the asymptotic analysis in Monkewitz *et al.* (2007),

$$\frac{\delta_{zpg}}{s} \sim 0.16 Re_s^{-1/7} \quad \text{and} \quad \frac{\theta_{zpg}}{s} \sim 0.016 Re_s^{-1/7}. \tag{1.1}$$

Choi & Moin (2012) postulated that instead of distributing the domain as a cube of side length determined by the average boundary layer thickness, the grid should be conformed to the local thickness of the boundary layer to maintain a fixed resolution in outer units (δ/Δ = constant, where δ is the boundary layer thickness and Δ is the

† Cadence Design Systems & ICME, Stanford

grid size). They reported that for WMLES, the grid points should scale linearly with the Reynolds number, $N_{pts}^{wm} \sim Re_x^1$. Thereafter, Yang & Griffin (2021) further revised the estimates for WRLES by utilizing outer-scale resolution scaling beyond the log-layer of an equilibrium turbulent boundary layer. Their grid-point estimates for WMLES were unchanged, however, with respect to Choi & Moin (2012). They also provided a cost-scaling estimate for using an explicit time-stepping scheme with the Reynolds number, or the number of time steps, N_t, which scale as $N_t \sim Re_x^{1/7}$.

While these previous studies have provided estimates for simulating equilibrium turbulent boundary layers, they have not considered the nonequilibrium effects imposed due to the effect of the pressure gradients. This problem is made more difficult since the effect of the pressure-gradient is nonlocal (Bobke *et al.* 2017), and the response of the boundary layer at a given Reynolds number and the nondimensional pressure-gradient (Clauser parameter, β) is dependent on the upstream history of the flow.

In this work, we follow the recent developments of Agrawal *et al.* (2023) to derive an approximate growth rate of the thickness of a turbulent boundary layer under the action of mild pressure gradients. The rest of this article is outlined as follows: Section 2 discusses a mathematical relationship between the boundary layer thickness, the pressure-gradient (dP/dx) and the momentum-thickness-based Reynolds number (Re_θ). Section 3 provides two examples of nonequilibrium flows for which the total number of grid points for performing WMLES are estimated. Section 4 offers some concluding remarks.

2. Grid-point and time-step estimates for WMLES of incompressible boundary layers experiencing pressure gradients

Fundamentally, a favorable or adverse pressure-gradient leads to a boundary layer that is thinner or thicker, respectively, than a corresponding (in Re_τ) zero-pressure-gradient boundary layer. One major factor that contributes to this is the response of the outer scales to a pressure-gradient (Bobke *et al.* 2017; Pozuelo *et al.* 2022). The previous efforts aimed at providing grid-point estimates for WMLES assumed grid resolutions that scale in outer flow units. The mean local shear is known to determine the dynamics of turbulence at different wall-normal locations in both equilibrium and nonequilibrium flows (Flores *et al.* 2007; Lozano-Durán & Bae 2019). As long as the pressure-gradient is not too strong, this shear rate is also nearly constant (across the outer region of the boundary layer) for nonequilibrium flows. Hence, a similar assumption about requiring a fixed outer resolution (δ/Δ) of the boundary layer may be motivated for nonequilibrium flows.

Agrawal *et al.* (2023) postulated an extension of Thwaites method (Thwaites 1949) to provide an ordinary differential equation for the growth of the momentum thickness (θ). The proposed relationships are provided below for completeness. Consider an x,y coordinate system where x is the streamwise direction and y is the wall-normal direction with $y = 0$ corresponding to the wall. For a turbulent boundary layer with freestream velocity distribution, $U_e(x)$, the authors proposed that

$$\frac{d\delta}{dx} \approx \frac{5}{200} + \frac{8}{200}m - \frac{U_e}{200\nu}\frac{d\theta^2}{dx} + \frac{d\delta zpg,corr}{dx}, \tag{2.1}$$

where $\delta_{zpg,corr}/x = 0.16Re_x^{-1/7} = 0.16(U_e x/\nu)^{-1/7}$. m is the Holstein-Bohlen parameter given as $m = \theta^2/\nu dU_e/dx$. The expression for the growth of the momentum thickness is another ordinary differential equation given as

$$\frac{d}{dx}(U_e^{C_m}\theta^2) \approx \nu C_c U_e^{C_m-1} + C_{Re,\infty} U_e^{C_m}\theta, \tag{2.2}$$

where $C_c = 1.45$, $C_m = 7.2$ and $C_{Re,\infty} = 0.0024$. Consider a turbulent boundary layer experiencing mild pressure gradients, such that it grows according to Eqs. (2.1) and (2.2). Let $\eta = \frac{x^*}{U_e^2}\frac{dP}{dx}$ be the parameter that governs the streamwise distance over which the pressure-gradient grows slowly (or remains locally constant). Bernoulli's principle implies that over the region $(0 - x^*)$,

$$U_e(x) = U_e^0\sqrt{1 - 2\frac{x^*}{U_e^{2,0}}\frac{dP}{dx}} \approx U_e^0(1-\eta). \tag{2.3}$$

Using this relation and the equations above, it can be shown that to the leading order (in η),

$$\frac{d\theta}{dx} \approx \left[\frac{C_c\nu}{2U_e^0\theta} + \frac{C_{Re,\infty}}{2}\right] + \left[\eta\left(\frac{C_c\nu}{2U_e^0\theta} + \frac{C_m\theta}{2x}\right)\right]. \tag{2.4}$$

Due to the proposed linear expansion in (m, Re_θ) space for the growth of the momentum thickness, the effect of the Reynolds number and the pressure-gradient on the growth of the boundary layer are explicitly separable. The terms in the first parentheses represent the growth rate of a zero-pressure-gradient (ZPG) boundary layer. Thus

$$\frac{d\theta}{dx} \approx \frac{d\theta^{zpg}}{dx} + \left[\eta\left(\frac{C_c\nu}{2U_e^0\theta} + \frac{C_m\theta}{2x}\right)\right]. \tag{2.5}$$

If the inviscid pressure-gradient distribution, $\eta = \eta(x)$, was known, then Eq. (2.5) could be integrated to give estimates for the growth of the boundary layer. If we further assume that the pressure gradients are sufficiently mild such that $\theta \approx \theta^{zpg} + \eta\frac{d\theta}{d\eta}\big|_{zpg}$, then the leading order expansion in η would yield

$$\frac{d\theta}{ds} \approx (0.016 + 0.6\eta)Re_x^{-1/7}. \tag{2.6}$$

Using Eqs. (2.1) and (2.6), an approximate relationship between the boundary layer thickness, δ [evaluated using the method of Griffin *et al.* (2021)] in (η, Re_x) space can be derived as

$$\delta(x) \approx \delta^{zpg} + 10^{-5}\eta x Re_x^{13/14} \approx 0.16 x Re_x^{-6/7} + 10^{-5}x[\frac{x}{U_e^{2,0}}\frac{dP}{dx}]Re_x^{13/14}. \tag{2.7}$$

In the asymptotic limit of a large Reynolds number, the model predicts that the boundary layer growth is determined linearly by the pressure-gradient, and slightly sublinearly by the Reynolds number. Following Choi & Moin (2012) and Yang & Griffin (2021), an integral relationship between δ and the total number of points required for performing WMLES is written as

$$N_{pts}^{wm} = N(x < x_0) + \int_{x_0}^{L_x}\int_0^{L_z}\frac{n_x n_y n_z}{\delta^2}dxdz, \tag{2.8}$$

where n_x and n_z are the number of points inside the boundary layer in the streamwise and spanwise directions, respectively. x_0 and L_x are the limits of the streamwise integral, and L_z is the domain size in the spanwise direction. Thus, for a given inviscid flow

distribution, the grid-point requirements for a boundary layer experiencing mild pressure gradients can be evaluated using Eqs. (2.7) and (2.8).

Finally, the time-step requirements for WMLES of nonequilibrium flows can also be determined. In practice, in WMLES, the time step is restricted due to the convective scales. Consider a time-stepping scheme that requires the Courant Friedrichs Lewy (CFL) number, $CFL < \mathcal{O}(1)$, for stability. This implies that

$$CFL = \frac{U\Delta t}{\Delta_x} < \mathcal{O}(1) \tag{2.9}$$

or

$$\Delta t < \frac{\Delta_x}{U} < \frac{\delta(x)}{n_x U} \leq \frac{\delta(x)}{n_x U_e(x)}. \tag{2.10}$$

The final inequality assumes that the streamwise velocity profile is at a maximum value at the edge of the boundary layer (ignoring any significant inviscid acceleration). Further, Eq. (2.10) needs to be satisfied globally in the boundary layer, forcing

$$dt \leq min_x[\frac{\delta(x)}{n_x U_e(x)}] = \frac{1}{n_x} min_x[\frac{\delta(x)}{U_e(x)}] = \frac{1}{n_x} min_x[\frac{0.16 x Re_x^{-6/7} + 10^{-5} x\eta Re_x^{13/14}}{U_e^0(1-\eta)}]. \tag{2.11}$$

For a flow with a prolonged favorable pressure-gradient, the downstream region of the flow controls the time-step requirements as the boundary layer thins and the outer scales become smaller. On the contrary, for a purely adverse pressure-gradient, the time step is constrained by the upstream flow.

3. Application to nonequilibrium flows

In this section, we consider two highly nonequilibrium flows to illustrate the use of the aforementioned estimates. Since a lower Reynolds number flow is more susceptible to a pressure-gradient, we first consider a low–Reynolds number NACA 4412 airfoil. Second, for flows experiencing a favorable pressure-gradient region followed by an adverse region, the boundary layer growth behaves differently compared to a ZPG estimate in different regions of the flow.

3.1. *Low–Reynolds number NACA 4412 airfoil*

The flow over the low–Reynolds number NACA 4412 airfoil (schematic presented in Figure 1) at a chord Reynolds number $Re_c = 0.1 \times 10^6$ simulated by Tanarro *et al.* (2020) is subject to an adverse pressure-gradient with the Clauser parameter, $\beta = \frac{\delta^* dP}{\rho U_e^2 dx} \approx 15$, at the trailing edge. A significant difference between the ZPG flow estimate of the boundary layer thickness and that from the proposed model is apparent in Figure 2(a). The total number of grid points, N_{pts}^{wm}, as a function of the streamwise distance is illustrated in Figure 2(b). The proposed model predicts that approximately 10% fewer grid points are needed within the boundary layer, while the boundary layer is also thicker, thereby reducing the number of points required in the inviscid flow, assuming a constant resolution in outer units (δ/Δ) is maintained globally. The reason for this minor reduction is primarily because the outer-units-based resolution is assumed to be sufficient to capture the flow phenomena accurately. Since the number of grid points scales locally with $1/\delta^2$ (see Eq. (2.8)), the grid-point requirements are set by the region for which δ is smaller, or the upstream region of the flow. Generally, since the effect of the pressure-gradient acts over some large streamwise distance, the upstream boundary layer thickness may

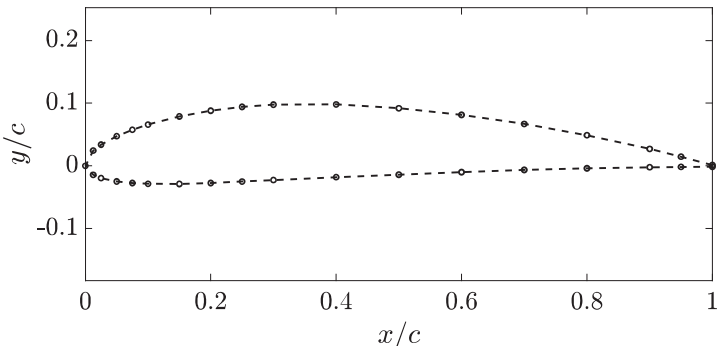

FIGURE 1. A schematic of the surface geometry of the NACA 4412 airfoil simulated in Tanarro *et al.* (2020). c is the chord length of the airfoil.

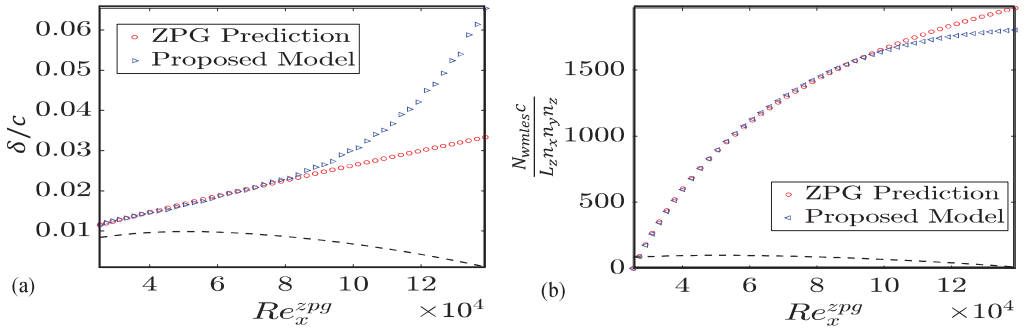

FIGURE 2. (a) The streamwise growth of the boundary layer thickness of NACA 4412 airfoil at $Re_c \approx 100,000$ and an angle of attack $\alpha = 5^o$ and (b) the streamwise Reynolds number dependence of the grid points required for WMLES. The ZPG estimate is derived from the freestream velocity at the first station. L_z and c are the spanwise extent and the chord length of the airfoil respectively; n_x, n_y and n_z are the number of points in the boundary layer in the streamwise, wall-normal and spanwise directions, respectively. The dotted lines in the subplots denote the geometry of the airfoil suction side surface.

remain relatively unaffected. Although not shown, the time-step requirement for WMLES of this flow is driven by the inlet δ and U_e, as the ratio δ/U_e increases thereafter (by approximately a factor of seven).

3.2. *Pre-separation region of the flow over the Boeing speed bump*

For flows that experience both a favorable and an adverse pressure-gradient, the growth of the boundary layer is at times smaller than a ZPG estimate, and then larger in other regions. An example of this is the flow over the Boeing speed bump (Williams *et al.* 2020; Gray *et al.* 2021) in which the flow accelerates and decelerates over a Gaussian-shaped bump before eventually separating off the surface. A schematic of the flow is provided in Figure 3. The pressure-gradient data (or equivalently, the C_p curve in the upstream region) from the quasi-DNS of Uzun & Malik (2022) is used in this work. Figure 4(a) shows the boundary layer growth predicted by the proposed model compared to a ZPG flow estimate. In Figure 4(b), the grid-point estimates are compared corresponding to these two boundary layer profiles. The total number of points from the new predictions is only 7% higher in the pre-separation region. However, the slope of the curve in Figure 4(b) is suggestive of a different distribution of the points in the domain; in the favorable

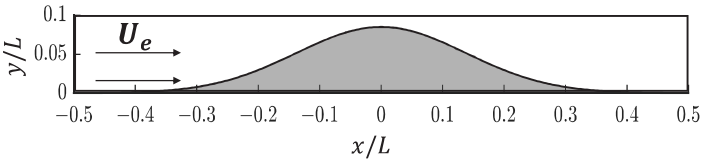

FIGURE 3. A schematic of the surface geometry over which the turbulent flow separates in the subsonic Boeing speed bump case of Uzun & Malik (2022). L is the characteristic length of the bump and U_e is the freestream flow velocity along the positive streamwise direction.

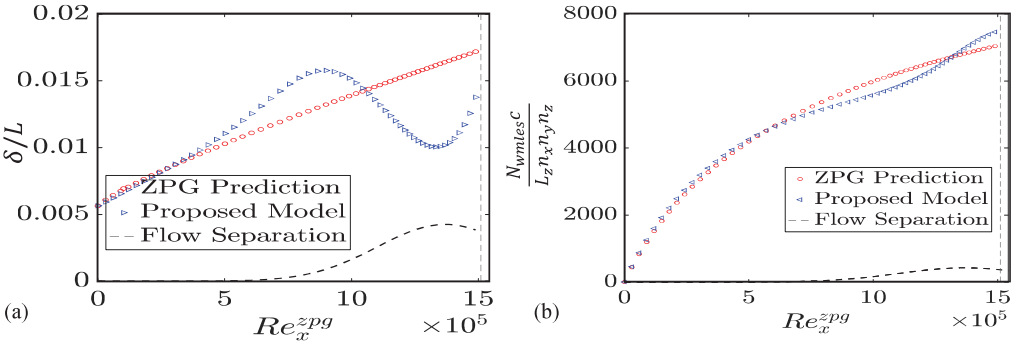

FIGURE 4. (a) The streamwise growth of the boundary layer thickness over the Boeing speed bump at $Re_L \approx 2 \times 10^6$ and (b) the streamwise Reynolds number dependence of the grid points required for WMLES. The ZPG estimate is derived from the freestream velocity at the first station. L_z and c are the spanwise extent and the chord length of the airfoil respectively; n_x, n_y and n_z are the number of points in the boundary layer in the streamwise, wall-normal and spanwise directions, respectively. Note that for this flow, the estimates are only plotted till the point of separation. The dotted lines in the subplots denote the geometry of the speed bump surface.

pressure-gradient region ($9 \times 10^5 \leq Re_x^{zpg} \leq 13 \times 10^5$), the boundary layer thins and more points are required locally, compared to a ZPG estimate. Conversely, in the adverse pressure-gradient regions ($5 \times 10^5 \leq Re_x^{zpg} \leq 9 \times 10^5$, $13 \times 10^5 \leq Re_x^{zpg} \leq 15 \times 10^5$), the boundary layer thickens and fewer number of points are needed. Figure 5 shows the local advective time step, $\Delta t = \delta(x)/U_e(x)$ from the proposed model for this flow with the maximum (in space) time-step is still imposed at the inflow. However, for a stronger pressure-gradient flow, the time step will likely be governed by the point of the minimum boundary layer thickness (within the favorable pressure-gradient region).

4. Concluding Remarks

In this article, the grid and time-step requirements for wall-modeled large-eddy simulation of nonequilibrium flows are explored using the recently developed extension of the Thwaites method in Agrawal *et al.* (2023). The analysis suggests a linear dependence of the boundary layer thickness on the applied pressure-gradient, and a slightly sublinear dependence on the Reynolds number, at least locally, for flows with strong nonequilibrium effects. The time-step estimates are also evaluated, and the results suggest that the convective time-step requirements may be set by the region of the strongest favorable pressure-gradient. For a flow with a unidirectional pressure-gradient, the time step is determined by the upstream region (for adverse pressure-gradients) and downstream re-

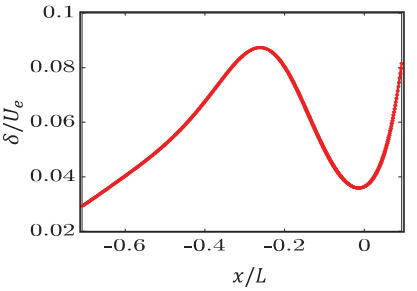

FIGURE 5. The streamwise growth of the advective time-step requirement for an explicit scheme with a stability criterion $CFL < 1$ for the flow over the Boeing speed bump at $Re_L \approx 2 \times 10^6$. Note that the δ in this plot corresponds to the prediction from the model in Eq. (2.7). This plot terminates at the point of flow separation, $x/L \approx 0.1$.

gion (for favorable pressure-gradients). Finally, for a low–Reynolds number NACA 4412 flow, and the flow over the Boeing speed bump (pre-separation), a minor difference of up to 10% in the total number of grid points is reported between the proposed estimates and the existing equilibrium flow-based estimates. Overall, only small differences were observed in the total number of grid points in comparison to a zero-pressure-gradient flow estimate.

Acknowledgments

This work was supported by NASA's Transformational Tools and Technologies project under grant number 80NSSC20M0201.

REFERENCES

AGRAWAL, R., BOSE, S. T., GRIFFIN, K. P. & MOIN, P. 2023 An extension of Thwaites method for turbulent boundary layers. arXiv:2310.16337 .

BOBKE, A., VINUESA, R., ÖRLÜ, R. & SCHLATTER, P. 2017 History effects and near equilibrium in adverse-pressure-gradient turbulent boundary layers. *J. Fluid Mech.* **820**, 667–692.

CHAPMAN, D. R. 1979 Computational aerodynamics development and outlook. *AIAA J.* **17**, 1293–1313.

CHOI, H. & MOIN, P. 2012 Grid-point requirements for large eddy simulation: Chapman's estimates revisited. *Phys. Fluids* **24**, 011702.

FLORES, O., JIMENEZ, J. & DEL ALAMO, J. C. 2007 Vorticity organization in the outer layer of turbulent channels with disturbed walls. *J. Fluid Mech.* **591**, 145–154.

GRAY, P. D., GLUZMAN, I., THOMAS, F., CORKE, T., LAKEBRINK, M. & MEJIA, K. 2021 A new validation experiment for smooth-body separation. In *AIAA Aviation 2021 Forum*, p. 2810.

GRIFFIN, K. P., FU, L. & MOIN, P. 2021 General method for determining the boundary layer thickness in nonequilibrium flows. *Phys. Rev. Fluids* **6**, 024608.

LOZANO-DURÁN, A. & BAE, H. J. 2019 Characteristic scales of Townsend's wall-attached eddies. *J. Fluid Mech.* **868**, 698–725.

MONKEWITZ, P. A., CHAUHAN, K. A. & NAGIB, H. M. 2007 Self-consistent high-

Reynolds-number asymptotics for zero-pressure-gradient turbulent boundary layers. *Phys. Fluids* **19**, 115101.

Nagib, H. M., Chauhan, K. A. & Monkewitz, P. A. 2007 Approach to an asymptotic state for zero pressure-gradient turbulent boundary layers. *Philos. T. R. Soc. A* **365**, 755–770.

Pozuelo, R., Li, Q., Schlatter, P. & Vinuesa, R. 2022 An adverse-pressure-gradient turbulent boundary layer with nearly constant $\beta \simeq 1.4$ up to $Re_\theta \simeq 8700$. *J. Fluid Mech.* **939**, A34.

Tanarro, Á., Vinuesa, R. & Schlatter, P. 2020 Effect of adverse pressure gradients on turbulent wing boundary layers. *J. Fluid Mech.* **883**, A8.

Thwaites, B. 1949 Approximate calculation of the laminar boundary layer. *Aeronaut. Quart.* **1**, 245–280.

Uzun, A. & Malik, M. R. 2022 High-fidelity simulation of turbulent flow past Gaussian bump. *AIAA J.* **60**, 2130–2149.

Williams, O., Samuell, M., Sarwas, E. S., Robbins, M. & Ferrante, A. 2020 Experimental study of a CFD validation test case for turbulent separated flows. In *AIAA Scitech 2020 Forum*, p. 0092.

Yang, X. I. A. & Griffin, K. P. 2021 Grid-point and time-step requirements for direct numerical simulation and large-eddy simulation. *Phys. Fluids* **33**, 015108.